

## Synthesis, Structure, and Complexation of a Large 28-mer Macrocyclic Containing Two Binding Sites for Either Anions or Metal Ions

Leroy Cronin,<sup>†</sup> Pamela A. McGregor,<sup>‡</sup> Simon Parsons,<sup>‡</sup> Simon Teat,<sup>§</sup> Robert O. Gould,<sup>‡</sup> Vivienne A. White,<sup>||</sup> Nicholas J. Long,<sup>||</sup> and Neil Robertson<sup>\*‡</sup>

Department of Chemistry, University of Glasgow, Glasgow G12 8QQ, Scotland, U.K., School of Chemistry, University of Edinburgh, Edinburgh EH9 3JJ, Scotland, U.K., CLRC Daresbury Laboratory, Daresbury, Warrington, Cheshire, U.K. WA4 4AD, and Department of Chemistry, Imperial College of Science Technology and Medicine, South Kensington, London, U.K. SW7 2AY

Received June 22, 2004

The “one-pot” synthesis and characterization of a large 28-mer macrocycle ( $H_4L^2$ ) with oxamido units capable of complexing guest ions through oxygen or nitrogen donor atoms is reported. Single-crystal structure determination of  $H_8L^2(NO_3)_4$  and  $\{Cu_2[H_2L^2](H_2O)_2\}(NO_3)_2$  demonstrated that the macrocycle contains two sites capable of complexing two nitrate anions or two copper(II) ions, involving a large structural reorganization in the conformation of the macrocyclic framework on coordination of the copper(II) ions when compared to the nitrate. Electrochemical and magnetic susceptibility measurements on the dinuclear Cu(II) complex and the related mononuclear and trinuclear Cu(II) complexes derived from the related 14-mer macrocycle were carried out and illustrate the role of the oxamido groups in mediating metal–metal interaction and delocalization.

### Introduction

The formation of multimetallic transition metal complexes offers an important route for the construction of new types of magnetic materials,<sup>1</sup> development of catalytic reagents,<sup>2</sup> models of metalloenzymes,<sup>3</sup> and the construction of metallosupramolecular architectures.<sup>4</sup> In all of these areas a key role is played by ligand control of metal oxidation state and reactivity, especially the interaction between the different metal centers. Strategies for the synthesis of multimetallic complexes have included the use of large macrocycles with

more than one binding site and also the linking of macrocycles through connecting units.

Large macrocycles comprising multiple metal binding sites can be formed when the metal itself is a unit in the backbone of the macrocycle<sup>5</sup> or when the macrocyclic unit is very rigid. For example, the use of Schiff-base condensation reactions using rigid precursors to minimize the formation of small cyclic products has been extensively exploited and in some cases these also incorporate binding sites featuring donor ligands that can bridge metal ions on complexation. Such complexes often have interesting properties due to the fact that the metal ions can be precisely positioned within the macrocyclic unit. Reduction of such Schiff-base species provides an example of the synthesis of flexible macrocycles in few steps,<sup>6</sup> although in other cases the synthesis of large flexible macrocycles comprising multiple metal binding sites can require a multistep synthesis.<sup>7</sup>

\* Author to whom correspondence should be addressed. E-mail: neil.robertson@ed.ac.uk.

<sup>†</sup> University of Glasgow.

<sup>‡</sup> University of Edinburgh.

<sup>§</sup> CLRC Daresbury Laboratory.

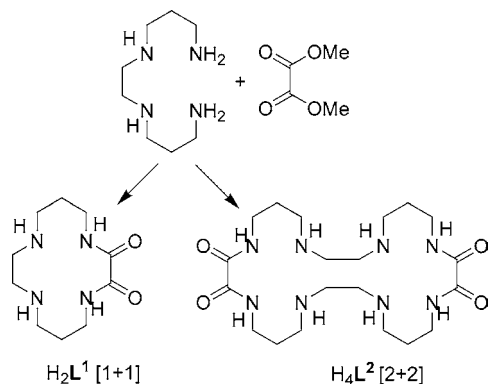
<sup>||</sup> Imperial College of Science Technology and Medicine.

- (1) Kahn, O. *Molecular Magnetism*; VCH Publishers Inc.: Weinheim, Germany, 1993. Kahn, O. *Adv. Inorg. Chem.* **1995**, *43*, 179. Kahn, O. *Acc. Chem. Res.* **2000**, *33*, 647. Murray, K. S. *Adv. Inorg. Chem.* **1996**, *43*, 261. Zhao, M.; Stern, C.; Barrett, A. G. M.; Hoffman, B. M. *Angew. Chem., Int. Ed.* **2003**, *42*, 462. Michel, S. L. J.; Hoffman, B. M.; Baum, S.; Barrett, A. G. M. *Prog. Inorg. Chem.* **2001**, *20*, 473. Mohanta, S.; Nanda, K. K.; Werner, R.; Haase, W.; Mukherjee, A. K.; Dutta, S. K.; Nag, K. *Inorg. Chem.* **1997**, *36*, 4656.
- (2) Fritsky, I. O.; Ott, R.; Pritzkow, H.; Krämer, R. *Chem.—Eur. J.* **2001**, *7*, 1221.
- (3) Torelli, S.; Belle, C.; Gautier-Luneau, I.; Pierre, J. L. *Inorg. Chem.* **2000**, *39*, 3526.
- (4) Seeber, G.; Kariuki, B. M.; Cronin, L. *Chem. Commun.* **2002**, 2912.

(5) Bodwin, J. J.; Cutland, A. D.; Malkani, R. G.; Pecoraro, V. L. *Coord. Chem. Rev.* **2001**, *216*, 489.

(6) Guerriero, P.; Tamburini, S.; Vigato, P. A. *Coord. Chem. Rev.* **1995**, *139*, 17; Cruz, C.; Carvalho, S.; Delgado, R.; Drew, M. G. B.; Felix, V.; Goodfellow, B. J. *Dalton Trans.* **2003**, 3172. Wang, Z.; Reibenspies, J.; Martell, A. E. *Inorg. Chem.* **1997**, *36*, 629. Drew, M. C. B.; Yates, P. C.; Esho, F. S.; Trocha-Grimshaw, J.; Lavery, A.; McKillop, K. P.; Nelson, J. J. *Chem. Soc., Dalton Trans.* **1988**, 2995. Cromie, S.; Launay, F.; McKee, V. *Chem. Commun.* **2001**, 1918.

(7) *Macrocyclic Synthesis*; David Parker, Ed.; Oxford University Press: Oxford, U.K., 1996.

**Scheme 1.** Synthesis of  $H_2L^1$  [1 + 1] and  $H_4L^2$  [2 + 2] Macrocycles<sup>a</sup>

<sup>a</sup> Variation of addition time allows an optimized yield of each product to be obtained, which can then be separated from the other cyclization products by washing and recrystallization. (N.B.: abbreviations  $H_2L^1$  and  $H_4L^2$  are used to refer to the *neutral* macrocycles, indicating the number of amide protons.)

Another approach to multinuclear complexes involves the tethering together of several macrocyclic units whereby each can separately complex a metal ion. This includes systems such as tethered cyclam macrocycles linked via short and long alkyl chains.<sup>8</sup> For systems with a flexible spacer, however, it can be difficult to control intermetallic interactions, and these may therefore be difficult to use in applications that exploit functional electronic properties of the system.

A few years ago we communicated the synthesis and characterization of a cyclam-based macrocyclic ligand that incorporated exogenous oxygen atoms arranged for chelation to a metal atom external to the macrocyclic ring.<sup>9</sup> Such ligands with deprotonatable amides are also related to amino acid based ligands.<sup>10</sup> This species was prepared through a straightforward cyclization procedure in one step using commercially available reagents (Scheme 1) and was shown to complex to Cu(II) ions giving both mononuclear and trinuclear complexes. Our initial report stimulated much further work using this macrocycle by ourselves and others, involving synthesis of heteropolynuclear complexes and assemblies.<sup>11</sup> The use of exogenous binding groups as bidentate linkers has been seldom utilized for the formation of multinuclear systems in macrocyclic chemistry. In addition to the macrocyclic complex  $Cu(II)L^1$ , we know of only one other report of metal macrocycle complexes that contain oxamido groups as bidentate linkers.<sup>12</sup> The potential of such

species to form novel functional materials however has been illustrated by the use of open chain oxamido analogues to form multinuclear complexes<sup>13–17</sup> and coordination polymers<sup>14,16–18</sup> with varied magnetic properties including ferromagnetic/antiferromagnetic complexes and ferrimagnetic chains. The extension of this approach to macrocyclic complexes offers the possibility to exploit the distinctions between macrocyclic systems and open-chain analogues, greater control over ligand selectivity, greater structural rigidity of the ligand framework, and greater thermodynamic and kinetic stability of the macrocyclic complexes.

In this paper we report the synthesis and characterization of the novel 28-membered macrocycle ( $H_4L^2$ ), an analogue of the 14-membered macrocycle ( $H_2L^1$ ) first communicated by us,<sup>9</sup> along with discussion of the series of mononuclear, dinuclear, and trinuclear Cu(II) systems based on these ligands including X-ray analysis of both nitro and Cu(II) complexes of the  $H_4L^2$  macrocycle. This represents the realization within a single straightforward synthetic platform of multimetallic species achieved through both a complex-as-ligand approach and also through a large-macrocycle approach.

## Experimental Section

Cyclic voltammetry was carried out using a standard three-electrode configuration with a Pt disk working electrode, platinum gauze counter electrode, and Ag/Ag<sup>+</sup> reference electrode against which the ferrocene/ferrocenium couple was found to be +0.13 V. Redox peaks in the text are reported against ferrocene/ferrocenium.  $[CuL^1]$  and  $[Cu(CuL^1)_2][BPh_4]_2$  were synthesized according to methods reported before.<sup>9</sup>

**Synthesis of  $H_4L^2$ .** *N,N'*-Bis(3-aminopropyl)ethylenediamine (1.65 mL, 9 mmol) in ethanol (200 mL) and dimethyl oxalate (1.06 g, 9 mmol) in ethanol (200 mL) were added dropwise simultaneously under N<sub>2</sub> via a peristaltic pump to 300 mL of refluxing ethanol. Complete addition took 32 h. The reaction mixture was allowed to reflux for a further 5 h and then left to cool. The white precipitate was filtered off and the filtrate reduced to dryness. The white residue was dissolved in hot propan-2-ol, hot filtered (to remove larger cycles), and left to stand overnight. The small amount of precipitate formed was filtered off. The filtrate was reduced to dryness and then taken up in dry acetonitrile. The less soluble 2 + 2 macrocycle was filtered off and dried under vacuum to yield 872 mg (29% yield). IR (cm<sup>-1</sup>, in KBr): 3300 s, 3550–3000 w, 2929 m, 2875 m, 1728 w, 1655 m, 1652 s, 1521 m, 1466 m, 1438 m, 1364 w, 1288 w, 1112 m, 1073 w, 767 m, 569 w. NMR (CDCl<sub>3</sub>, 270 MHz,  $\delta$ ): 1.74 (m, 8H, NCH<sub>2</sub>CH<sub>2</sub>CH<sub>2</sub>N); 2.75 (m, 16H, RHNCH<sub>2</sub>); 3.38 (q, 8H, (O)CNHCH<sub>2</sub>,  $J = 5.7$  Hz); 8.66 (br NH); 9.08 (br NH). Positive ion FAB MS:  $m/z = 457$  (MH<sup>+</sup>). Anal.

- (8) McAuley, A.; Subramanian, S. *Coord. Chem. Rev.* **2000**, 200–202, 75.
- (9) Cronin, L.; Mount, A. R.; Parsons, S.; Robertson, N. *J. Chem. Soc., Dalton Trans.* **1999**, 1925.
- (10) McDonald, M. R.; Scheper, W. M.; Lee, H. D.; Margerum, D. W. *Inorg. Chem.* **1995**, 34, 229.
- (11) Kou, H.-Z.; Zhou, B. C.; Gao, S.; Wang, R.-J. *Angew. Chem., Int. Ed.* **2003**, 42, 3288. Tang, J.-K.; Si, S.-F.; Wang, L.-Y.; Liao, D.-Z.; Jiang, Z.-H.; Yan, S.-P.; Cheng, P.; Liu, X. *Inorg. Chim. Acta* **2003**, 343, 288. Tang, J.-K.; Si, S.-F.; Wang, L.-Y.; Liao, D.-Z.; Jiang, Z.-H.; Yan, S.-P.; Cheng, P.; Liu, X. *Inorg. Chem. Commun.* **2002**, 5, 1012. Tang, J.-K.; Si, S. F.; Gao, E.-Q.; Liao, D.-Z.; Jiang, Z.-H.; Yan, S.-P. *Inorg. Chim. Acta* **2002**, 332, 146. Tang, J.-K.; Wang, L.-Y.; Zhang, L.; Gao, E.-Q.; Liao, D.-Z.; Jiang, Z.-H.; Yan, S.-P.; Cheng, P. *J. Chem. Soc., Dalton Trans.* **2002**, 1607. Tang, J.-K.; Li, Y.-Z.; Wang, Q.-L.; Gao, E.-Q.; Liao, D.-Z.; Jiang, Z.-H.; Yan, S.-P.; Cheng, P.; Wang, L.-F.; Wang, G.-L. *Inorg. Chem.* **2002**, 41, 2188. Kou, H.-Z.; Zhou, B. C.; Wang, R.-J. *Inorg. Chem.* **2003**, 42, 7658.

- (12) Gao, E.-Q.; Bu, W.-M.; Yang, G.-M.; Liao, D.-Z.; Jiang, Z.-H.; Yan, S.-P.; Wang, G.-L. *J. Chem. Soc., Dalton Trans.* **2000**, 1431.
- (13) Escuer, A.; Vicente, R.; Ribas, J.; Costa, R.; Solans, X. *Inorg. Chem.* **1992**, 31, 2627.
- (14) Benelli, C.; Fabretti, A. C.; Giusti, A. *J. Chem. Soc., Dalton Trans.* **1993**, 409. Kahn, O.; Journaux, Y.; Sletten, J. *Inorg. Chem.* **1986**, 25, 439.
- (15) Sanada, T.; Suzuki, T.; Kaizaki, S. *J. Chem. Soc., Dalton Trans.* **1998**, 959.
- (16) Fukita, N.; Ohba, M.; Shiga, T.; Okawa, H.; Ajiro, Y. *J. Chem. Soc., Dalton Trans.* **2001**, 64.
- (17) Kahn, O. *Prog. Inorg. Chem.* **1995**, 179.
- (18) Sanz, J. L.; Cervera, B.; Ruiz, R.; Bois, C.; Faus, J.; Lloret, F.; Julve, M. *J. Chem. Soc., Dalton Trans.* **1996**, 1359.

Calcd for  $C_{20}H_{40}N_8O_4$ : C, 52.61; H, 8.83; N, 24.64. Found: C, 53.01; H, 9.20; N, 24.25.

**Synthesis of  $[H_2L^1]$ .** Dimethyl oxalate (2.140 g, 18 mmol) was dissolved in ethanol (350 mL), and freshly distilled  $N,N'$ -bis(3-aminopropyl)ethylenediamine (3.145 g, 18 mmol) was dissolved in ethanol (350 mL). The two solutions were then added dropwise under nitrogen with stirring to refluxing ethanol (50 mL) via a peristaltic pump. Complete addition took 2 weeks. After cooling, the cloudy precipitate was filtered off and discarded as a polymeric byproduct. The filtrate was reduced to dryness and the resultant white solid dissolved in hot propan-2-ol, hot filtered, cooled, and refiltered. The filtrate was reduced to dryness and the sticky white solid taken up in acetone. The 2 + 2 macrocycle was removed by filtration and the filtrate reduced to dryness to yield the 1 + 1 product  $[H_2L^1]$  (3.11 mmol, 17.3% yield). Mp: 138–140 °C. Positive ion FAB mass spectrometry:  $m/z$  229 ( $MH^+$ ).  $^1H$  NMR ( $CDCl_3$ ,  $\delta$ ): 1.10 (multiplet, 4H,  $^3J_{HH}$  5.454,  $NHCH_2CH_2CH_2NHC(O)$ ); 2.57 (s, 4H,  $NHCH_2CH_2NH$ ); 2.75 (dt, 4H,  $^3J_{HH}$  5.211  $CH_2CH_2NHC(O)$ ); 3.49 (t, 4H,  $^3J_{HH}$  5.45,  $NHCH_2CH_2NH$ ); 8.42 (br, 2H,  $NH$ ); 8.87 (br d, 2H,  $NHC(O)$ ).

**Synthesis of  $[H_8L^2(NO_3)_4]$ .** An aqueous solution of  $H_4L^2$  [2 + 2] (0.25 g, 0.5 mmol in 5 mL of water) was acidified to a pH 3–4 by slow addition of 1 M solution of  $HNO_3$ . Slow evaporation of the solution over a number of days yielded crystals suitable for X-ray diffraction (0.075 g, 0.145 mmol, 26%). IR ( $cm^{-1}$ , Golden Gate): 3300 s, 3550–3000 w, 2929 m, 2875 m, 1728 w, 1655 m, 1652 s, 1521 m, 1466 m, 1438 m, 1364 w, 1301 vs, 1280 vs, 1112 m, 1073 w, 1065 m, 1045 m, 991 m, 952 m, 901 m, 870 m, 826 s, 702 m, 681 m, 640 w, 513 s.  $^1H$  NMR ( $DMSO-d_6$ , 400 MHz,  $\delta$ ): 1.06 (m, 8H,  $NCH_2CH_2CH_2N$ ); 2.09 (m, 16H,  $RHNCH_2$ ); 2.6 (m, 8H,  $(O)CNHCH_2$ ). Positive ion FAB MS:  $m/z$  = 457 ( $MH^+$ ). Anal. Calcd for  $C_{20}H_{44}N_{12}O_{16}$ : C, 33.88; H, 6.26; N, 23.72. Found: C, 34.22; H, 5.89; N, 23.42.

**Synthesis of  $[Cu_2H_2L^2][NO_3]_2$ .** A methanol solution of  $H_4L^2$  [2 + 2] (0.05 g, 0.1 mmol in 5 mL of MeOH) was added to an aqueous solution of potassium hydroxide (0.012 g, 0.2 mmol in 1 mL of water), and then a methanolic solution of copper(II) nitrate was added (0.065 g, 0.22 mmol in 2 mL of MeOH). Addition of the copper(II) nitrate caused an instant color change from colorless to deep blue. Filtration of the solution followed by crystallization by slow evaporation yielded the complex as a crystalline product over several days (0.018 g, 0.024 mmol, 22%). IR ( $cm^{-1}$ , Golden Gate, in KBr): 3630–3000 m, 3434 m, 3240 m, 2950 m, 2870 m, 1650 b, s, 1433 s, 1398 w, 1352 m, 1342 m, 1316 m, 1259 w, 1174 m, 1092 b, s, 1015 m, 991 w, 939 w, 886 w, 816 w, 626 m, 541 w, 502 w. Anal. Calcd for  $C_{20}H_{38}N_{10}O_{10}Cu_2 \cdot 3H_2O$ : C, 31.66; H, 5.85; N, 18.47. Found: C, 31.42; H, 6.02; N, 18.89.

Crystal data for  $C_{40}H_{88}N_{16}O_8 \cdot 8NO_3 \cdot 4H_2O$ :  $M_r$  = 780.7; triclinic, space group  $P\bar{1}$ ;  $a$  = 11.595(3),  $b$  = 11.803(6),  $c$  = 14.5754(7) Å;  $\alpha$  = 89.86(5),  $\beta$  = 83.68(5),  $\gamma$  = 64.05(4)°;  $V$  = 1780.5(4) Å<sup>3</sup>;  $Z$  = 2; 12 280 reflections measured, 9063 unique which were collected on Station 9.8 at the SRS Daresbury Laboratory, Daresbury, U.K., with a Bruker Smart system ( $\lambda$  = 0.6884 Å) and used in all calculations. The structure was solved with SHELXS-97 and refined with SHELXL-97,<sup>19</sup> and the structure converged to  $R1$  = 0.120 ( $I > 2\sigma(I)$ ) and  $wR2$  = 0.366 (all data) and goodness-of-fit = 1.062 on all  $F^2$  (9063 data; 500 parameters; 29 restraints; residuals in the final map = +0.706/−0.566 e Å<sup>−3</sup>).

Crystal data for  $C_{40}H_{76}N_{16}Cu_2 \cdot 4NO_3 \cdot 15H_2O$ :  $M_r$  = 1681.6; monoclinic, space group  $P2_1/c$ ;  $a$  = 24.8634(6),  $b$  = 18.046(10),  $c$

= 15.977(13) Å;  $\beta$  = 96.93(5)°;  $V$  = 7116.2(4) Å<sup>3</sup>;  $Z$  = 4;  $\mu(Mo K\alpha)$  = 1.837 mm<sup>−1</sup>; 10 438 reflections measured on a Stoe Studi-4 diffractometer operating with Cu K $\alpha$  radiation, 5415 unique which were used in all calculations. The structure was solved with SHELXS-97 and refined with SHELXL-97,<sup>19</sup> and the structure converged to  $R1$  = 0.134 ( $I > 2\sigma(I)$ ) and  $wR2$  = 0.396 (all data) and goodness-of-fit = 1.071 on all  $F^2$  (5415 data; 417 parameters; 372 restraints; residuals in the final map = +1.177/−0.966 e Å<sup>−3</sup>). It is important to note that the crystals were very weakly diffracting and the quality of this determination is low; however, the connectivity is well established.

## Results and Discussion

**(i) Synthesis and Structural Properties.** We have isolated the  $H_4L^2$  macrocycle as the [2 + 2] reaction product using the same precursors that give rise to  $H_2L^1$  [1 + 1] (Scheme 1) through separate optimization of the reaction conditions for each macrocycle. Rapid addition of the acyclic reagents gives a mixture of [1 + 1], [2 + 2], [3 + 3], and higher cycles and polymer as evidenced by mass spectrometry. The formation of  $H_2L^1$  is favored by high-dilution conditions, and we were able to synthesize this species in 17% yield through dropwise addition of the two reagents using a peristaltic pump over 14 days. Through use of a method involving addition of the reagents at a more rapid rate (32 h), we obtained a satisfactory yield (29%) of the [2 + 2] product  $H_4L^2$ . In each reaction scheme the product was obtained in the presence of other cyclization/polymerization products; however, use of a washing and recrystallization scheme allowed the separate isolation of each macrocycle. This was confirmed by mass spectroscopic analysis, and we have shown by studies with the pure [1 + 1] product, the pure [2 + 2] product, and known mixtures of the two that, in this case, mass spectroscopic studies do give an indication of purity. Thus, both  $H_2L^1$  and  $H_4L^2$  were each readily obtained from a one-pot synthesis from commercial reagents in satisfactory yield and purity without the need for column chromatography. The ease of synthesis is particularly striking for the novel ligand  $H_4L^2$  where preparation of such a large flexible macrocycle with multiple binding sites often involves a multistep reaction.<sup>7</sup> It is apparent that  $H_2L^1$  and  $H_4L^2$  may adopt different conformations in solution due to the greatly increased flexibility of  $H_4L^2$  compared with  $H_2L^1$ , and these differences are reflected in the NMR parameters shown for the two macrocycles in chloroform solution. This also allowed an additional convenient method to verify that each macrocycle was isolated without significant contamination from the other.

The structural characterization of  $[H_8L^2(NO_3)_4]$  using single-crystal X-ray crystallography was accomplished after it was discovered that the macrocycle complexes with nitrate anions.<sup>20</sup> Accurate structural determination was difficult due to the small crystal size; however, the results were sufficient to establish the connectivity and overall geometry of the species. This structural analysis reveals that the nitrate–

(19) Sheldrick, G. M. *SHELXS-97 and SHELXL-97, Programs for Crystal Structure Solution and Refinement*; Universität Göttingen: Göttingen, Germany, 1997.

(20) Initial NMR titrations have shown that the  $H_4L^2$  does complex with nitrate anions in solution, and binding constants with nitrate and other anions/competition studies will be reported later.

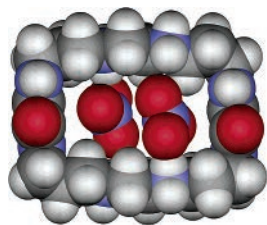


**Figure 1.** (a) Space-filling representation of the framework of the  $L^2$  macrocycle from the crystal structure of the  $[H_8L^2(NO_3)_4]$  [2 + 2] macrocycle. Color scheme: white = hydrogen; gray = carbon; red = oxygen; blue = nitrogen. The view shows the protonated macrocycle  $[H_8L^2(NO_3)_2]^{2-}$  and the two nitrate ions that are included in the cavity, with the two remaining nitrate ions omitted.

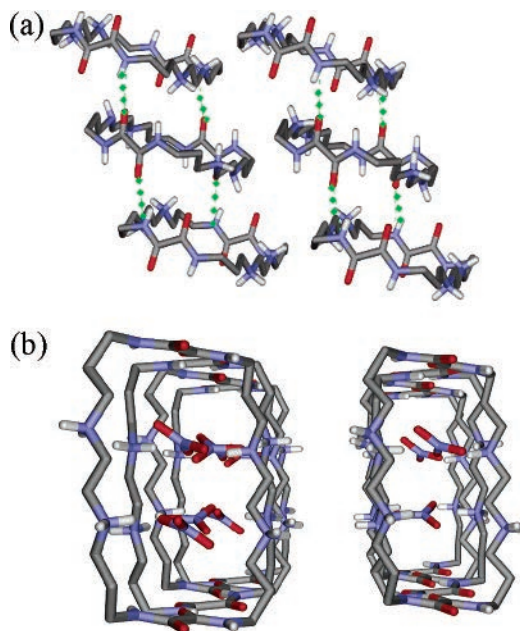


**Figure 2.** (a) Representation of the packing arrangement of the [2 + 2] macrocycle in the solid state (atom color scheme as for Figure 1). The hydrogen bonding between the macrocycles is depicted by green dotted lines. The solvent and counterions are omitted in these representations. (b) Representation of the packing arrangement of the [2 + 2] macrocycle in the solid state (atom color scheme as for Figure 1) viewed to show the channels of nitrate anions.

macrocycle complex has a remarkable rectangular structure giving rise to a cavity. In this case the cavity is filled by two nitrate anions (Figure 1). The rectangular cavity is ca. 7.4 Å wide and 11.4 Å long, and the two nitrate anions are pressed against the two walls across the macrocycle, in close contact with the two  $-NH_2^+$  moieties on the opposite side of the ring at distances which range 2.72–2.98 Å indicating two hydrogen-bonded interactions/nitrate anion. In addition, the nitrate anions are stacked next to each other at a distance 3.5 Å and also against the two planar amino moieties at either side of the cavity at a distance of ca. 4 Å, indicating a weak  $\pi$ - $\pi$  interaction between the nitrate anions (Figure 1).

Examination of the packing interactions between the macrocycles reveals that they are stacked in a staggered arrangement which allows hydrogen bonding between the *exo* oxygen atoms of the amino groups (at distances between 2.79 and 2.84 Å) in one macrocycle with the  $-NH-$  moieties of the amino groups with another macrocycle (Figure 2a). This is similar to the hydrogen-bonded arrangement that is found between adjacent peptide chains hydrogen-bonded to

a  $\beta$ -sheet in many proteins.<sup>21</sup> Furthermore the area occupied by the nitrate anions within the macrocycle appear to form stacks comparable to that of an ion channel when viewed down the axis of the stacked macrocycles (Figure 2b).<sup>22</sup>

Cyclic polyamide molecules have previously been widely studied as receptors for a variety of anions including species such as carboxylates, halides, phosphonates, acetates, and sulfates as well as nitrates.<sup>23</sup> Among these studies, we are aware of only one previous structural characterization of a receptor that contains two associated nitrate anions, and this is based on a receptor with the appropriate 3-fold symmetry to accommodate the nitrate anion.<sup>24</sup> This resulted in a separation between nitrogen atoms within the two anions of 3.339(4) Å, which compares with a distance of 3.591 Å in the structure of  $[H_8L^2(NO_3)_2]^{2-}$ . A related solution study of the same literature system, however, indicated that the incorporation of two nitrates in the host was not reproduced at any significant concentration in solution where the 1:1 host:guest complex dominated, stressing the importance of solution-binding studies in the assessment of receptors for anions.<sup>25</sup>

Complexation of  $H_4L^2$  in methanol with copper(II) nitrate in the presence of 2 equiv of sodium hydroxide causes an instant color change to a deep blue solution indicating complexation of the ligand with the copper(II) ions. In addition to the normal analytical studies indicating the formation of a complex of the form  $\{Cu_2[H_2L^2](H_2O)_2\}-(NO_3)_2$ , crystallization of the complex allowed analysis by single-crystal X-ray crystallography and confirmed that the ligand is able to ligate two copper(II) ions (Figure 3). Although the single crystals obtained were of limited quality, the structure obtained again allows the unambiguous determination of the connectivity and basic geometry of the system. There are two crystallographically independent complexes/unit cell, and the structural analysis shows that the macrocycle binds each copper(II) ion in a  $\{N_3O\}$  coordination environment where two of the nitrogen donors are derived from the secondary amino groups (Cu–N distances range 1.933(6) and 2.045(5) Å) and the third is a deprotonated amide nitrogen (Cu–N distances range between 1.946(5) and 1.974(6) Å). In addition, the amide oxygen from the macrocycle is the fourth donor atom (Cu–O distances range 1.933(6) and 1.980(5) Å) and the coordination sphere of the 5-coordinate copper(II) ion is completed by a water molecule (Cu–OH<sub>2</sub> distances range 2.266(8) and 2.455(8) Å). The two water molecules on each copper(II) ion also hydrogen bond to each other at a distance of ca. 2.8 Å, and the Cu–Cu distances are 6.079 and 6.239 Å (Figure 3). The possibility for a flexible amide containing macrocycle to coordinate to a metal ion through either the N or O atom

(21) Schneider, J. P.; Pochan, D. J.; Ozbas, B.; Rajagopal, K.; Pakstis, L.; Kretsinger, J. *J. Am. Chem. Soc.* **2002**, *124*, 15030.

(22) Green, D.; Pace, S.; Curtis, S. M.; Sakowska, M.; Lamb, G. D.; Dulhunty, A. F.; Casarotto, M. G. *Biochem. J.* **2003**, *370*, 517.

(23) Bondy, C. R.; Loeb, S. J. *Coord. Chem. Rev.* **2003**, *240*, 77.

(24) Mason, S.; Clifford, T.; Seib, L.; Kuczera, K.; Bowman-James, K. *J. Am. Chem. Soc.* **1998**, *120*, 8899.

(25) Hynes, M. J.; Maubert, B.; McKee, V.; Town, R. M.; Nelson, J. J. *Chem. Soc., Dalton Trans.* **2000**, 2853.

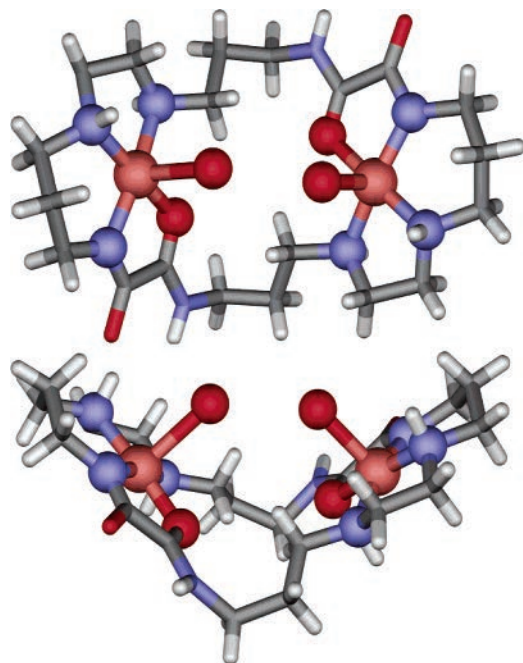


**Figure 3.** Representation of the crystal structure of  $\{\text{Cu}_2[\text{H}_2\text{L}^2](\text{H}_2\text{O})_2\}-(\text{NO}_3)_2$  in the solid state (atom color scheme as in Figure 1). The solvent and counterions are omitted in these representations.

depending on acidity of the solution has been previously described.<sup>26</sup>

Furthermore, it is interesting to note that the coordination of the copper(II) ions cause the 4 macrocyclic donor atoms to form a square plane to within a deviation of not greater than 0.1 Å (average deviation is 0.06 Å). The consequence of this coordination has a marked effect on the conformation of the macrocycle. The complexed macrocycle can be seen to “fold-up” from the uncomplexed planar unit so that a V-shaped cleft is formed where the two diverging arms of the V are formed by the planar  $\{\text{CuN}_3\text{O}\}$  units in each “arm” of the macrocycle. The angle formed between the intersection of these planes is ca. 110°. These V-shaped units pack together to form “ribbonlike” strands which are connected (Figure 4) via a 3-dimensional hydrogen-bonded network that involves both solvent water molecules and the nitrate anions in addition to the macrocycles.

The structure of the dinuclear Cu(II) complex is reminiscent of the field of cascade chemistry. This involves the formation of binuclear systems with metals such as Cu(II) where a free coordination site on each metal results in the sequential binding of an ambidentate or bridging anion that links the two metal centers.<sup>27</sup> The binding of water molecules linked via a hydrogen bond to the otherwise square planar Cu(II) centers creates a similar structural motif and suggests that this binuclear Cu(II) complex would be interesting to explore in reactions with appropriate anions that might replace the water molecules.

**(ii) Electrochemical and Magnetic Properties.** The electronic properties of the new complex  $\{\text{Cu}_2[\text{H}_2\text{L}^2](\text{H}_2\text{O})_2\}-(\text{NO}_3)_2$

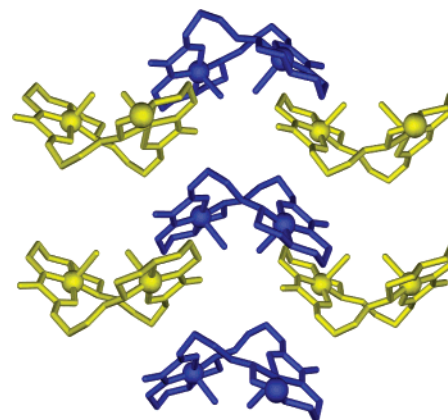


**Figure 4.** Representation of the packing arrangement of the V-shaped complex  $\{\text{Cu}_2[\text{H}_2\text{L}^2](\text{H}_2\text{O})_2\}^{2+}$  in the solid state. Alternate units are colored blue and yellow, and the metal ions are shown as the large spheres. The solvent and counterions are omitted.

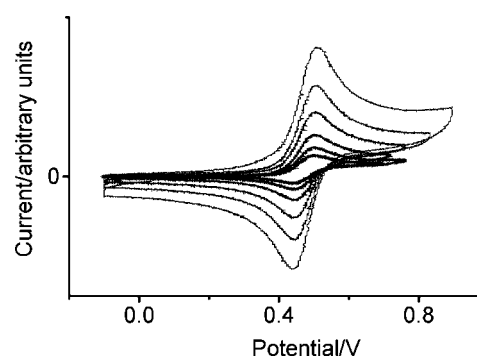


**Figure 5.** Cyclic voltammogram of  $[\text{CuL}^1]$  in  $\text{CH}_3\text{CN}/0.1 \text{ M LiClO}_4$  at 5, 10, 20, 50, 100, and 200  $\text{mV s}^{-1}$ .

$(\text{NO}_3)_2$  were investigated and compared with those of  $[\text{CuL}^1]$  and  $[\text{Cu}(\text{CuL}^1)_2][\text{BPh}_4]_2$ , for which some brief preliminary studies were carried out.<sup>9</sup> The complexes  $[\text{CuL}^1]$ ,  $[\text{Cu}(\text{CuL}^1)_2][\text{BPh}_4]_2$ , and  $\{\text{Cu}_2[\text{H}_2\text{L}^2](\text{H}_2\text{O})_2\}(\text{NO}_3)_2$  were all investigated by cyclic voltammetry in  $\text{CH}_3\text{CN}$ .  $[\text{CuL}^1]$  showed a redox process at +0.47 V (Figure 5). The forward and reverse peak heights were equivalent, separated by 65 mV, and showed no scan rate dependence, and peak height varied as the square root of scan rate with no scan rate dependence of peak positions. On this basis, the process was assigned as the chemically and electrochemically reversible Cu(II)/Cu(III) redox couple. This is consistent with previous observations that inclusion of alkyl substituents in Cu(III) amido species stabilizes the ligand against degradation through hydrolysis.<sup>28</sup> Related cyclam-based macrocycles are known with oxygen atoms substituted in nonchelating positions,<sup>29</sup> and it is interesting to note, in comparison, that electrochemical study of the related bis(*exo*-O<sub>2</sub>-cyclam) macrocycle with the oxygen atoms in the nonchelating 5 and 7 positions gives a Cu(II)/Cu(III) redox couple at +0.15 V

(26) Inoue, M. B.; Velazquez, E. F.; Ruiz-Lucero, A.; Inoue, M.; Raitsimring, A.; Fernando, Q. *Inorg. Chem.* **1999**, *38*, 834.

(27) Amendola, V.; Fabbrizzi, L.; Mangano, C.; Pallavicini, P.; Poggi, A.; Taglietti, A. *Coord. Chem. Rev.* **2001**, *219–221*, 821.

(28) Ruiz, R.; Surville-Barland, C.; Aukauloo, A.; Anxolabehere-Mallart, E.; Journaux, Y.; Cano, J.; Munoz, M. C. *J. Chem. Soc., Dalton Trans.* **1997**, 745. Cervera, B.; Sanz, J. L.; Ibanez, M. J.; Vila, G.; lloret, F.; Julve, M.; Ruiz, R.; Ottenwaelder, X.; Aukauloo, A.; Poussereau, S.; Journaux, Y.; Cano, J.; Munoz, M. C. *J. Chem. Soc., Dalton Trans.* **1998**, 781.

(29) Fremont, L.; Espinosa, E.; Meyer, M.; Denat, F.; Guillard, R.; Huch, V.; Veitch, M. *New J. Chem.* **2000**, *24*, 959.

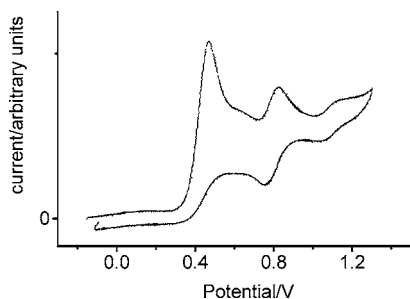


**Figure 6.** Cyclic voltammogram of  $[\text{Cu}(\text{CuL}^1)_2][\text{BPh}_4]_2$  in  $\text{CH}_3\text{CN}/0.1 \text{ M LiClO}_4$  at  $50 \text{ mV s}^{-1}$  scanning to positive potential.

(vs  $\text{Fc}/\text{Fc}^+$ ),<sup>30</sup> despite the identical donor set and size of the ligand. In this context, it is important to recognize that  $[\text{CuL}^1]$  shows no appreciable solubility in  $\text{CH}_3\text{CN}$  in the absence of the electrolyte  $\text{LiClO}_4$  or with an alternative electrolyte such as  $[\text{N}^n\text{Bu}_4][\text{PF}_6]$ . It is apparent that the solubility of  $[\text{CuL}^1]$  is dependent on interaction between the chelating *exo*-O atoms and the  $\text{Li}^+$  ions of the electrolyte and that this interaction leads not only to dissolution of the complex but also to a large shift to more positive potential of the  $\text{Cu(II)}/\text{Cu(III)}$  couple, consistent with an increase in positive charge density communicated to the Cu center through the delocalized amido bridge.

The complex  $[\text{Cu}(\text{CuL}^1)_2][\text{BPh}_4]_2$  showed three oxidation processes (Figure 6). The first of these, a chemically irreversible oxidation at  $+0.47 \text{ V}$ , arises from the  $[\text{BPh}_4]^-$  counterion. The subsequent two oxidations were observed to be chemically and electrochemically reversible with half-wave potentials of  $+0.80$  and  $+1.08 \text{ V}$  and were assigned as oxidations of the  $\text{Cu(II)}$  centers within the complex. The first oxidation showed a peak height approximately twice as large as the second and on this basis and the more comparable potential to the  $\text{Cu(II)}/\text{Cu(III)}$  couple for  $[\text{CuL}^1]$  was assigned as the  $\text{Cu(II)}/\text{Cu(III)}$  redox process for the outer two metal centers of  $[\text{Cu}(\text{CuL}^1)_2]^{2+}$ . This process is shifted to more positive potential in comparison with oxidation of  $[\text{CuL}^1]$  suggesting a stronger influence of the central  $\text{Cu(II)}$  ion in comparison with the influence of  $\text{Li}^+$  ions from the electrolyte on  $[\text{CuL}^1]$ . The redox process at  $+1.08 \text{ V}$  was assigned as the  $\text{Cu(II)}/\text{Cu(III)}$  couple for the central  $\text{Cu(II)}$  of the complex. It is interesting to note the reversibility of this couple, which again suggests a delocalized system extending across the central Cu and the ligands consistent with the approximately planar geometry previously observed for this complex.<sup>9</sup> Scanning to negative potential revealed peaks corresponding to the irreversible reduction at  $-1.2 \text{ V}$  and associated oxidation peak at  $-0.67 \text{ V}$  that we previously observed in our preliminary account of the electrochemistry of the complex.<sup>9</sup> It is interesting to note that in our earlier study we did not observe either of the Cu-based oxidation processes determined here for this species. This may be due to the fact that the earlier work was carried out on a hydrated nitrate salt where the X-ray structure revealed the terminal  $\text{Cu(II)}$  species to be five coordinate with one  $\text{H}_2\text{O}$  ligand. We found that addition of small quantities of water to the

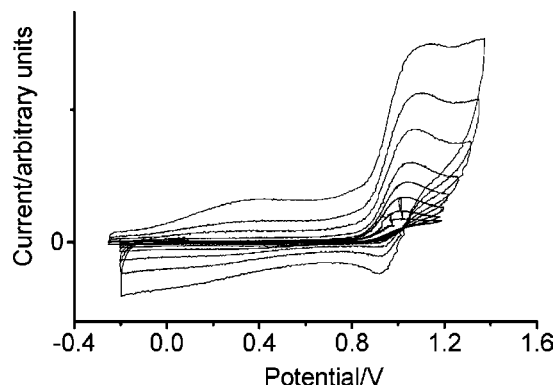


**Figure 7.** Cyclic voltammogram for  $\{\text{Cu}_2[\text{H}_2\text{L}^2](\text{H}_2\text{O})_2\}^{2+}$  in  $\text{CH}_3\text{CN}/0.1 \text{ M LiClO}_4$  at 10, 20, 50, 100, 200, 1000, and 2000  $\text{mV s}^{-1}$ .

solution of  $[\text{Cu}(\text{CuL}^1)_2][\text{BPh}_4]_2$  led to the loss of the oxidation peaks for the complex although the exact mechanism for the change in behavior is not known.

In contrast, the cyclic voltammogram for complex  $\{\text{Cu}_2[\text{H}_2\text{L}^2](\text{H}_2\text{O})_2\}^{2+}$  (Figure 7) showed a chemically irreversible oxidation process with a peak potential of  $+1.05 \text{ V}$ . Increase in scan rate showed a small change in the oxidation peak position toward more positive potential, and at rapid scan rates (e.g.  $1000 \text{ mV s}^{-1}$ ) a small return reduction peak was observed at  $+0.92 \text{ V}$ . Clearly this  $\text{Cu(III)}$  complex cannot be stabilized to the same extent as the mononuclear and trinuclear species. This may arise from a combination of factors that might include the increased overall positive charge on the dinuclear complex, the different coordination mode ( $\text{N}_3\text{O}$ ) for the binuclear species, a reduced level of electronic delocalization between the  $\text{Cu(II)}$  center and the ligand, and more facile hydrolysis of the ligand by  $\text{Cu(III)}$  for the dinuclear species.

The complexes  $[\text{CuL}^1]$  and  $\{\text{Cu}_2[\text{H}_2\text{L}^2](\text{H}_2\text{O})_2\}(\text{NO}_3)_2 \cdot 3.5\text{H}_2\text{O}$  have been investigated as powder samples by magnetic susceptibility measurement over the temperature range  $2\text{--}300 \text{ K}$  and the data corrected for a diamagnetic contribution estimated by Pascal's constants. Data for the mononuclear complex  $[\text{CuL}^1]$  were fit by the Curie–Weiss expression giving a Curie constant of  $0.381 \text{ emu K mol}^{-1}$ , consistent with one  $g = 2.03$  unpaired electron, and a Weiss constant of  $-1.5 \text{ K}$ . This shows the presence of only weak antiferromagnetic interactions suggesting that magnetic coupling between  $\text{Cu(II)}$  centers in adjacent macrocycles is not mediated by any particularly efficient coupling pathway. The complex  $\{\text{Cu}_2[\text{H}_2\text{L}^2](\text{H}_2\text{O})_2\}(\text{NO}_3)_2 \cdot 3.5\text{H}_2\text{O}$  also showed Curie–Weiss behavior with a Curie constant of  $0.822 \text{ emu K mol}^{-1}$ , consistent with two  $g = 2.19$   $\text{Cu(II)}$  centers/molecule, and a Weiss constant of  $-0.06 \text{ K}$ . This indicates completely negligible coupling between the two  $\text{Cu(II)}$  centers within the macrocycle, consistent with the large  $\text{Cu–Cu}$  distance and the lack of any discernible superexchange pathway that would facilitate interaction between the metal centers.

The results for both the mononuclear and dinuclear complexes contrast greatly with our previously reported magnetic properties of  $[\text{Cu}(\text{CuL}^1)_2][\text{ClO}_4]_2$ ,<sup>8</sup> where a coupling of  $J = -364.2 \text{ cm}^{-1}$  was determined between the

(30) Fabbrizzi, L.; Perotti, A.; Poggi, A. *Inorg. Chem.* **1983**, *22*, 1412.

### A 28-mer Macrocyclic Containing Two Binding Sites

central Cu(II) and outer Cu(II) centers within the trinuclear complex. In this example, magnetic exchange was mediated by the oxamido group through the approximately planar, delocalized bridging unit, whereas, for the mononuclear and dinuclear complexes, it is clear that no efficient magnetic exchange pathways operate.

#### Conclusions

We have synthesized and isolated a 28-membered macrocycle possessing both N- and O-donor atoms within oxamido units, related to the 14-membered macrocycle we have previously reported. The macrocycle has been crystallographically characterized in two separate structures with either 2 Cu(II) or 2 NO<sub>3</sub><sup>-</sup> units coordinated within the deprotonated or protonated large macrocyclic framework, respectively. The electrochemical and magnetic properties of the dinuclear Cu(II) complex are reported and compared with studies on the related mononuclear and trinuclear Cu(II) complexes derived from the related 14-membered macrocycle. All of these macrocycles contain *exo*-O<sub>2</sub> bridging units

that can link metal centers, and clear evidence of the importance of electronic communication through these is evidenced by the Cu(II)/Cu(III) redox couples in the mononuclear and trinuclear species, plus the variation in magnetic properties for the three complexes. The realization of strong intermetallic interaction through the oxamido bridging unit was not observed for the macrocycle H<sub>4</sub>L<sup>2</sup> in the way that was previously determined for H<sub>2</sub>L<sup>1</sup>, although this possibility may be realized by future work. Further studies will examine the 28-membered macrocycle as a possible anion/small molecule receptor and will extend the coordination chemistry toward other metal centers and polymetallic assemblies.

**Acknowledgment.** We thank the Leverhulme Trust and EPSRC for funding.

**Supporting Information Available:** Crystallographic data in CIF format. This material is available free of charge via the Internet at <http://pubs.acs.org>.

IC049190V